

## Investigation of a Postprocessing Method to Tailor the Mechanical Properties of Carbon Nanotube/Polyamide Fibers

Genevieve Palardy,<sup>1</sup> David Trudel-Boucher,<sup>2</sup> Pascal Hubert<sup>1</sup>

<sup>1</sup>Department of Mechanical Engineering, McGill University, 817 Sherbrooke Street West, Montreal, Quebec, H3A 0C3, Canada

<sup>2</sup>Industrial Materials Institute, National Research Council Canada, 75 de Mortagne, Boucherville, Quebec, J4B 6Y4, Canada

Correspondence to: P. Hubert (E-mail: pascal.hubert@mcgill.ca)

**ABSTRACT:** The incorporation of carbon nanotubes to thermoplastic fibers can potentially improve mechanical, thermal and electrical properties. In this article, a methodology to tailor the mechanical properties of carbon nanotube/nylon fibers is presented. Multi-walled nanotubes (MWNT) were combined to polyamide 12 through melt compounding and twin-screw extrusion. Pellets containing between 0 and 5.0 wt % MWNT were extruded and subsequently melt spun with a capillary rheometer to produce filaments. To further promote the alignment of the polymer chains and MWNTs, postdrawing parameters were systematically investigated: temperature, drawing speed and elongation. The best improvements in terms of elastic modulus and yield strength were measured at 140°C and 500% elongation, whereas drawing speed was shown to have a negligible effect. It was confirmed through electron microscopy and X-ray diffraction that these enhancements were mainly induced by the alignment of the polymer chains along the fibers' axis.

© 2013 Wiley Periodicals, Inc. *J. Appl. Polym. Sci.* 130: 4375–4382, 2013

**KEYWORDS:** nanostructured polymers; polyamides; fibers; extrusion; mechanical properties

Received 27 March 2013; accepted 26 June 2013; Published online 20 July 2013

DOI: 10.1002/app.39713

### INTRODUCTION

Over the past decades, there have been significant advancements toward the development and manufacturing of synthetic fibers with exceptional mechanical properties. The main reason for their improved properties is the alignment and stretching of the polymer chains which was perfected through specific manufacturing techniques developed over the years.<sup>1–3</sup> Further improvement now lies in the reinforcement of the fibers themselves by using microparticle or nanoparticle. In the past two decades, carbon nanotubes (CNT) have been studied as reinforcing materials and have shown to improve mechanical, thermal and electrical properties.<sup>1,4</sup>

One of the main methods to further improve the mechanical properties of thermoplastic fibers is postdrawing. It consists of stretching the fibers, generally through a series of ovens and winders at varying velocities, to enhance the alignment of the polymer chains and consequently, increase the mechanical properties. This process has been extensively studied for conventional thermoplastic fibers, especially for melt spinning.<sup>2,3,5</sup> However, this is not the case for CNT/thermoplastic fibers and most studies solely investigated the effect of the draw ratio (DR).

A certain number of papers were published regarding the effect of postdrawing on various thermoplastic fibers reinforced with

single-walled and multiwalled nanotubes (SWNT and MWNT).<sup>6–16</sup> Haggenueller et al.<sup>7,8</sup> found that the draw ratio increased tensile strength, but did not have a significant effect on the elastic modulus or the alignment of CNTs for MWNT/polymethyl methacrylate (PMMA) fibers. Houphouet-Boigny studied these properties in more details with melt spun polypropylene (PP) fibers containing 1.0–4.0 wt % of MWNT.<sup>9</sup> Fibers were postdrawn at room temperature according to three different winding speeds (360, 720, and 1500 mm/min) and results were similar to Haggenueller et al. Modulus of elasticity data did not show any particular trend, but a maximum increase of 600% in tensile strength was measured for the highest DR values and CNT contents. Based on transmission electron microscopy (TEM) and two-dimensional X-ray diffraction patterns, a preferential alignment of the CNTs was qualitatively observed along the fibers axis. More recently, studies published by Mazinani et al. and Sulong et al. reported data on cold-drawn MWNT/polyethylene (PE) and MWNT/polyethylene terephthalate (PET) fibers, showing that mechanical drawing did not significantly influence the properties, regardless of CNT content.<sup>10,11</sup> Young's modulus, tensile strength and elongation at break slowly decreased with an increase of DR. An opposite trend was observed in previous studies from Haggenueller et al. and Houphouet-Boigny, but this behavior was explained by the fact that the crystallinity and alignment of the polymer

© 2013 Wiley Periodicals, Inc.

chains were reduced by the presence of nanofillers. In these cases, it was therefore possible to stretch the fibers at higher draw ratios.

It is expected that postdrawing at high temperature would however lead to better results as it would allow the polymer chains and nanotubes to move and rearrange themselves more easily. A certain number of studies reported such a trend for MWNT/nylon 12 and SWNT/PET fibers.<sup>14,15</sup> Perrot et al. measured modulus and yield strength values as high as double those for unreinforced nylon 12 fibers with a maximum draw ratio of 7. Similar DR values were reached for SWNT/PET filaments, which led to a maximal increase of 500% in the elastic modulus with 2.0 wt % SWNT. Moore et al. however published contradicting results for CNT/PP fibers.<sup>16</sup> The addition of CNTs mostly led to worse elastic modulus and tensile strength values, before and after hot drawing. Explanations were not provided for the loss of mechanical properties, but it was suggested that the nanotubes interacted differently depending on the type of PP matrix used.

Overall, postdrawing of CNT/thermoplastic fibers at high temperature is a promising way to enhance the alignment of the nanotubes and reach impressive values in terms of tensile strength and Young's modulus. There is still, however, a lack of rigorous investigation to identify the key factors leading to optimum results for CNT/thermoplastic fibers, as it is assumed that draw ratio is the sole contributor to the properties enhancement.

In this article, a systematic investigation of the postdrawing parameters on the morphology and tensile properties of MWNT/polyamide 12 fiber will be presented. Fibers containing between 0 and 5 wt % MWNT were melt spun, then postdrawn at different temperature, speed and elongation values. The drawing speed, within the values investigated, did not have a significant effect on the mechanical properties. It was observed, however, that higher temperature and elongation values had the greatest impact on the Young's modulus and yield strength. Transmission electron microscopy (TEM), wide-angle X-ray diffraction (XRD) and differential scanning calorimetry (DSC) experiments were carried out to understand the contribution from the polymer chains alignment, crystallinity and the state of dispersion of the nanotubes.

## EXPERIMENTAL

### Materials and Extrusion

Rilsan® polyamide 12 (PA12) pellets and Graphistrength C M1-20 masterbatch were provided by Arkema. The general molecular structure of PA12 is shown on Figure 1. The masterbatch was mixed with polyamide 12 pellets through melt compounding using a twin-screw industrial extruder to produce pellets with lower CNT contents of 1.0, 2.0, and 5.0 wt %. A total quantity of 500 g was generated for each MWNT weight fraction. A masterbatch of pure PA12 was also prepared under the same thermal conditions for comparison. The temperature was kept at 200°C with twin screws RPM between 200 and 202. The polymer strand at the exit of the die was cooled in a water bath and pelletized for subsequent characterization and processing.

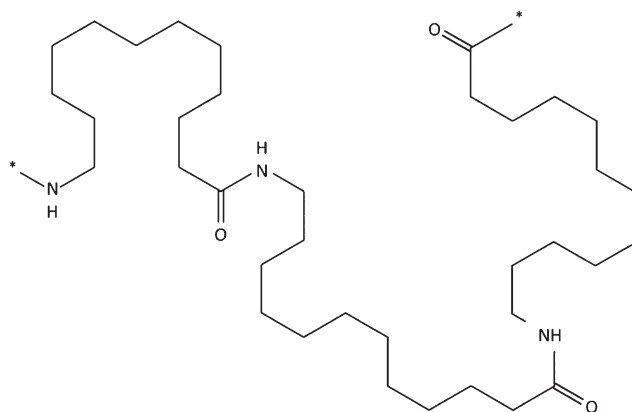


Figure 1. Molecular structure of polyamide 12.

Prior to each processing step, the material was put in a drying oven at 80°C under vacuum for at least 48 h.

Nanocomposite pellets containing 0, 1.0, 2.0, and 5.0 wt % MWNT were extruded with a *Rosand* capillary rheometer. A quantity of 50–60 g was spun for each masterbatch through a die with a 1-mm diameter hole. The speed of the piston was set at 10 mm/min and the fibers were collected at a speed of 152 m/min. A 7.6-cm diameter roller was located 45 cm below the extrusion die. The fibers' diameters varied between 110 and 200  $\mu\text{m}$ , with corresponding draw ratios from 25 to 83.

### Morphological Analyses

**SEM and TEM.** The fibers' surface was observed with an SEM-JEOL at a voltage of 5.0 kV. They were coated with gold at an accelerating voltage of 2.0 kV. The dispersion of the nanotubes was qualitatively assessed through TEM (Philips CM200 200kV). Filaments were transversally cut at an angle of approximately 30°. The samples were prepared by cryo-microtomy (−100°C) using a Leica Ultracut UCT microtome. Slices with a thickness of 80 nm were cut at a speed of 0.6 mm/s and collected on copper grids.

**X-ray Diffraction.** A General Area Detector Diffraction System (GADDS), from Bruker AXS Inc., was used to perform 2D wide-angle X-ray scattering (WAXS) experiments. Small bundles of fibers were mounted on a rectangular aluminum frame and positioned 8.94 cm from the detector. This position allowed for  $2\theta$  values between approximately 4° and 28°. The exposure time was set to 120 s and the radiation source was made of copper with a wavelength,  $\lambda$ , of 1.54 Å.

**Differential Scanning Calorimetry.** A TA Instruments Q100 differential scanning calorimeter was used to determine the crystallinity of fiber samples before and after postdrawing, in the range of 0–210°C at a rate of 10°C/min.

### Postdrawing and Mechanical Testing

Postdrawing was performed with a *Brückner* biaxial stretching machine. Fiber samples of 115 mm in length were cut and individually clamped in the machine at room temperature. The effects of drawing temperature, speed, and elongation were investigated. Three different temperatures were chosen: 100, 120, and 140°C. Those values were selected because they are

above  $T_g$  but below the melting temperature of the nanocomposites. It was observed, through preliminary tests, that the samples would stick to the clamps of the stretching machine above 140°C. Based on those preliminary tests, drawing speeds of 1, 3, and 5 m/min, and elongation values of 300 and 500%, were selected. A total of 128 fibers were stretched, but drawing speeds and final elongations higher than 5 m/min and 500%, respectively, were not always attainable without breakage for all CNT contents.

Tensile tests were performed with an *Instron 5548 Microtester* machine with a load cell of 5N. A gauge length of 25 cm and a cross-head speed of 5 mm/min were chosen. To perform tensile tests, fiber samples of approximately 50 cm in length were cut and fixed to a paper frame with epoxy glue, according to the ASTM standard D3379-75.

After mounting the fibers on paper frames, their diameter was measured with a Nikon Eclipse L150 optical microscope at a magnification of 10 $\times$ . Measures were taken at three points along the length, at a distance of approximately 5 mm from each other. The average value was used for tensile tests. Between 5 and 10 fiber samples were tested for each set of postdrawing parameter and MWNT weight fraction.

## RESULTS AND DISCUSSION

### Morphological Analysis

Before postdrawing, the fibers' surface exhibited a smooth texture with a uniform diameter, regardless of CNT content, as shown on Figure 2(a). After postdrawing, stretching lines formed on the surface of the PA12 matrix, as seen on Figure 2(b), indicating effective drawing in the direction of the fiber's axis (arrow).

Figure 3 shows representative TEM images for fibers containing 5.0 wt % MWNT before postdrawing (a) and after postdrawing until 300% (b) and 500% elongation (c) at 140°C. The black arrows indicate the direction of the fibers' axis. A close-up in Figure 3(b) shows the nanotubes more clearly. Small agglomerates and entanglements were present before and after postdrawing, but their distribution was generally uniform. As for the alignment of the MWNTs, visual analysis of several TEM pictures revealed that it remained quite low, even at 500% elongation.

### X-ray Diffraction

XRD experiments were performed on selected postdrawn fibers according to the following parameters for each temperature: (a) 300% elongation and 3 m/min, and (b) 500% elongation and 1 m/min. Figure 4 illustrates a representative distribution of 2D WAXS patterns for MWNT contents of 0, 1.0, and 5.0 wt %. The vertical arrows indicate the fiber's axis. The patterns exhibited a strong alignment of the polymer chains toward that axis. Sharp diffraction peaks were observed along the equatorial axes for the (200) plane of the  $\gamma$  phase of nylon 12, as reported in the literature.<sup>17–21</sup> As the elongation increased, the diffraction peaks were sharper and less diffused along the circumference. Because of the low MWNT concentration, it was however not possible to distinguish any peaks corresponding to the nanotubes.

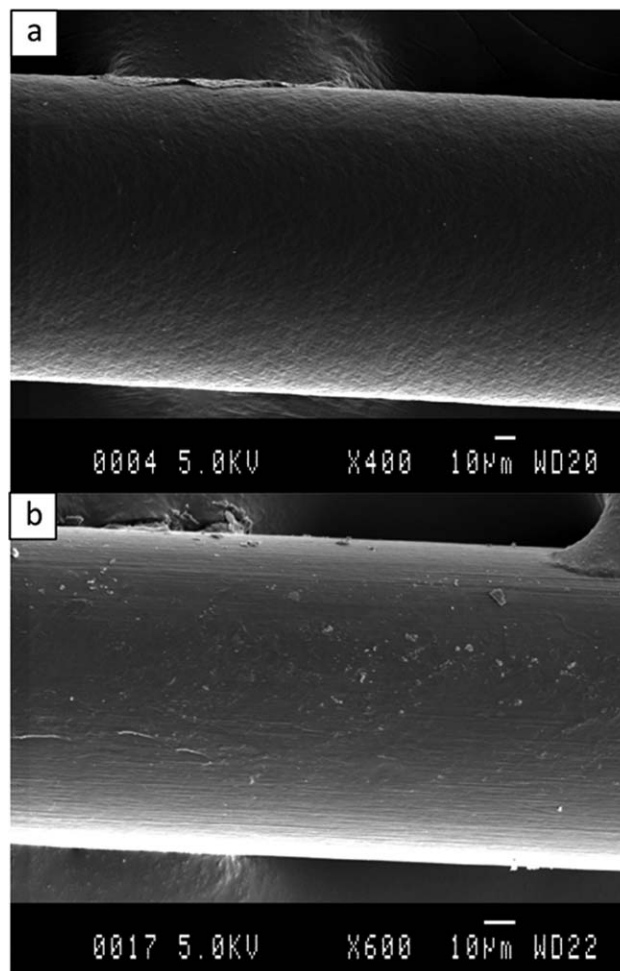


**Figure 2.** SEM image of a PA12 fiber containing 2.0 wt % MWNT before (a) and after postdrawing at 140°C until 500% elongation (b). The arrow in (b) indicates the direction of the fiber's axis.

To quantify the effect of the nanotubes and postdrawing conditions on the alignment of the polymer chains, the intensity distribution of the  $\gamma(200)$  plane was extracted for azimuthal angles,  $\varphi$ , between 0° and 360°. A Gaussian fit was performed on the data with PeakFit 4.12 software and the full width at half maximum (FWHM) was calculated for both peaks at  $\varphi = 90^\circ$  and  $\varphi = 270^\circ$ . The average FWHM values are reported on Figure 5 for as-spun and postdrawn fibers containing between 0 and 5.0 wt % MWNT. For as-spun fibers, a decrease in FWHM with MWNT content suggests that CNTs encourage the alignment of the chains. Several studies in the literature presented similar findings, explaining that the nanotubes act as a template for polymer orientation along the fiber's axis.<sup>6,22–25</sup> FWHM dramatically decreased between as-spun and post-drawn fibers, but the values remained relatively stable when MWNT content increased from 0 to 5.0 wt %. This behavior shows that CNTs do not contribute to further alignment after drawing above 300% elongation. In the literature, Perrot et al. investigated the effect of spinning conditions on the FWHM of polymer chains for PA12 fibers containing 7 wt % MWNT.<sup>14</sup> Their values were comprised between 8.5° and 34.3°, which is consistent with the

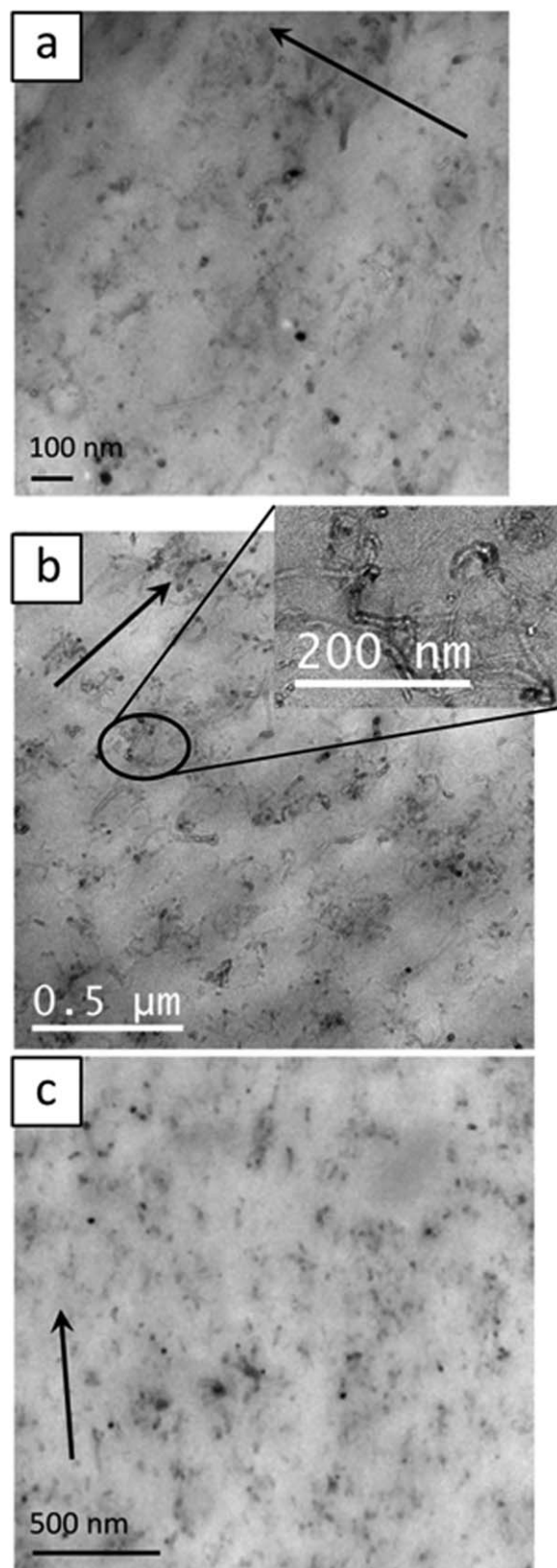


**Figure 3.** Transversal TEM images of PA12 fibers containing 5.0 wt % MWNT before postdrawing (a) and postdrawn until 300% (b) and 500% (c) elongation at 140°C. The black arrows show the direction of the fibers' axis.

results from Figure 5 for similar draw ratios after postdrawing. A wider range of CNT weight fractions and postdrawing parameters were however not investigated.

### Crystallinity

For thermoplastic fibers, crystallinity directly influences their mechanical properties and it is therefore important to determine if it is affected by the inclusion of nanotubes. The crystallinity ( $X_c$ ) of fibers before and after postdrawing was determined by DSC. Samples postdrawn at all temperatures, until 300% at 1 m/min were selected for the experiments.  $X_c$  was calculated from the DSC curves with eq. (1):

$$X_c(\%) = \frac{\Delta H_m}{(1 - W_{\text{CNT}})\Delta H_m^0} \times 100 \quad (1)$$

where  $\Delta H_m$  is the melting enthalpy,  $W_{\text{CNT}}$  is the weight fraction of CNTs and  $\Delta H_m^0$  is the melting enthalpy of a 100% crystalline sample of PA12.<sup>9</sup>  $\Delta H_m^0$  was chosen as 209.2 J/g, a theoretical value used in the literature.<sup>19,26</sup> Figure 6 shows that the crystallinity of the fibers before (dashed line) and after postdrawing decreases when CNT weight fraction increases, regardless of postdrawing temperature. The values range between 33.1 and 25.4% and are close to what was previously reported in the literature for DSC measurements.<sup>20</sup> This particular decreasing trend was also observed in other studies where CNTs did not promote nucleation.<sup>22,27–30</sup> The lack of alignment and exfoliation of the nanotubes along the fibers' axis, as well as crystallization rate during cooldown, might be causes for lower crystallinity.

### Tensile Properties

Figure 7 shows typical engineering stress–strain curves for samples postdrawn at 100°C, 300% elongation (a), 120°C, 300% elongation (b) and 140°C, 500% elongation (c). The drawing speed is 1 m/min for all temperatures. Results are shown for samples containing 0, 1.0, 2.0, and 5.0 wt % MWNT. The black curves represent pure PA12 fibers before postdrawing. Tensile curves for PA12 fibers typically exhibit a linear elastic region, followed by yield and a considerable plastic deformation before break. At all temperatures, improvements in terms of Young's modulus ( $E$ ) and yield strength ( $\sigma_y$ ) were observed as MWNT content increased. This behavior is consistent with what was previously reported in the literature for PA12/CNT fibers.<sup>14,20,21,26</sup> The inclusion of nanotubes, however, induced lower strain-to-failure values, and consequently, strain energy density, indicating an increase in brittleness, especially after 500% elongation [Figure 7(c)]. Similar results were also reported by Sandler et al.,<sup>26</sup> Perrot et al.,<sup>14</sup> and Chatterjee et al.<sup>20</sup> for PA12/MWNT fibers with elongation at break ranging between 10 and 325%. Weakened polymer-nanotube interface and inclusions creating defects in the polymer chains were identified as some of the main causes.<sup>31</sup> In this work, CNT agglomerates and randomly aligned nanofillers were observed by TEM, even after 500% elongation [Figure 3(c)], confirming that they could act as imperfections and lead to lower strain-to-failure.

To adequately compare the results and eliminate dimensional effects, the average  $E$  values were plotted with draw ratio on

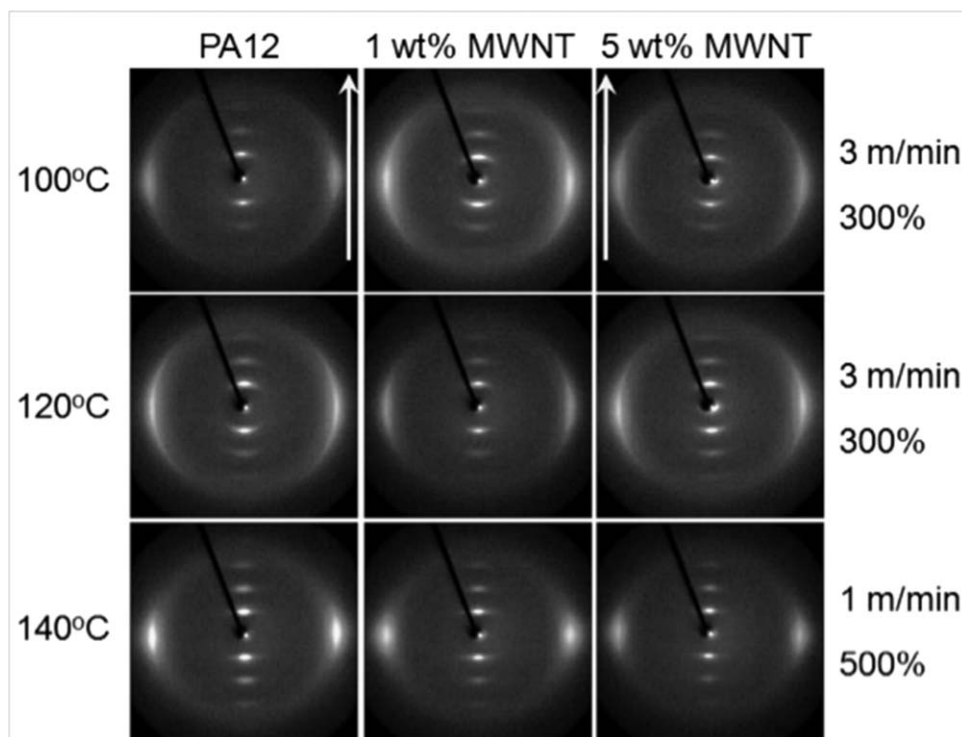


Figure 4. 2D WAXS patterns for MWNT/PA12 fibers postdrawn at 100, 120, and 140°C, at 1 and 3 m/min until 300 and 500% elongation.

Figure 8 for all for all postdrawing temperatures, elongations and speeds. The results were divided into three sections:

1. Lower left corner: as-spun fibers (before drawing);
2. Centered dashed rectangle: fibers postdrawn at 300% elongation, at 1, 3, and 5 m/min;
3. Upper right corner dashed rectangle: fibers postdrawn at 500% elongation, at 1, 3, and 5 m/min.

Drawing speeds of 5 m/min could only be reached at 140°C. Moreover, the drawing speed, within the range investigated, did not influence the elastic modulus according to a specific trend.

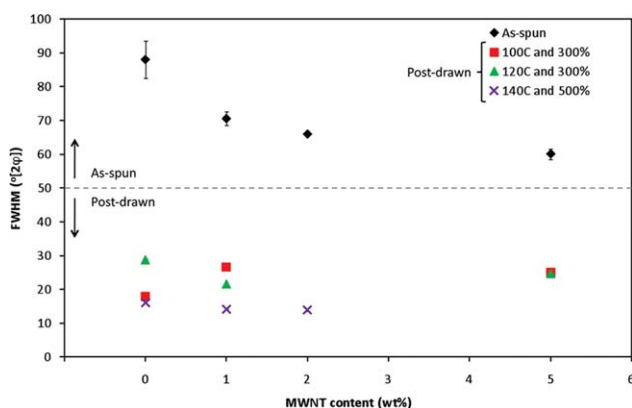


Figure 5. FWHM of as-spun and postdrawn PA12 fibers containing 0, 1.0, 2.0, and 5.0 wt % MWNT. Error bars for postdrawn fibers are smaller than the markers. [Color figure can be viewed in the online issue, which is available at wileyonlinelibrary.com.]

The values are therefore not identified on Figure 8. Figure 8(a) shows the results for postdrawn fibers at 100°C. After 300% elongation, the elastic modulus ranged between 1.2 and 1.7 GPa. Highest values were obtained for pure PA12 fibers and samples containing 1.0 wt %. At 100°C, it was only possible to stretch fibers until 500% elongation for those containing 0 and 2.0 wt % MWNT, at 1 m/min. Nanocomposite fibers exhibited the best elastic modulus with 3.7 GPa.

Figure 8(b) shows the average  $E$  for post-drawn fibers at 120°C. After 300% elongation, the elastic modulus slightly increased

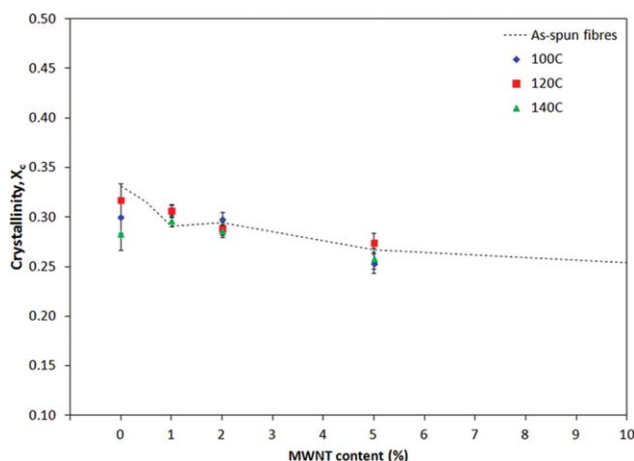
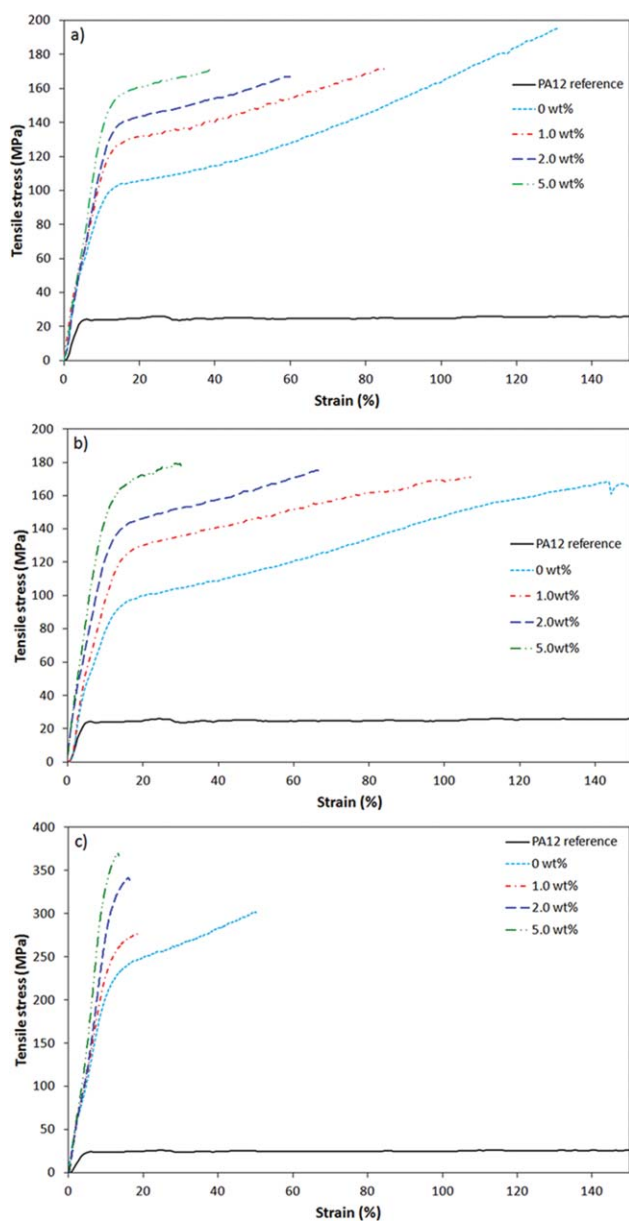


Figure 6. Comparison between calculated crystallinity of as-spun fibers before and after postdrawing at 100, 120, and 140°C (300% elongation, 1 m/min). [Color figure can be viewed in the online issue, which is available at wileyonlinelibrary.com.]



**Figure 7.** Typical stress–strain curves on postdrawn fibers containing 0, 1.0, 2.0 and 5.0 wt % MWNT, under the following conditions: for (a) Final elongation = 300%, speed = 1 m/min, 100°C, (b) Final elongation = 300%, speed = 1 m/min, 120°C, and (c) Final elongation = 500%, speed = 1 m/min, 140°C. [Color figure can be viewed in the online issue, which is available at [wileyonlinelibrary.com](http://wileyonlinelibrary.com).]

compared to 100°C and is between 1.4 and 1.8 GPa. Fibers containing 2.0 and 5.0 wt % MWNT possess a higher elastic modulus than pure PA12 filaments. However, there was no clear influence of the nanotubes weight fraction. Highest  $E$  value was obtained at 500% elongation, 3.1 GPa, which was only possible to achieve with samples containing 2.0 wt % MWNT, at 1 m/min.

Figure 8(c) shows the average  $E$  for postdrawn fibers at 140°C. After 300% elongation, the data points were more scattered and for similar DR, showed an increase with MWNT content, from 1.0 to 5.0 wt %. The values were located between 1.5 and 2.2

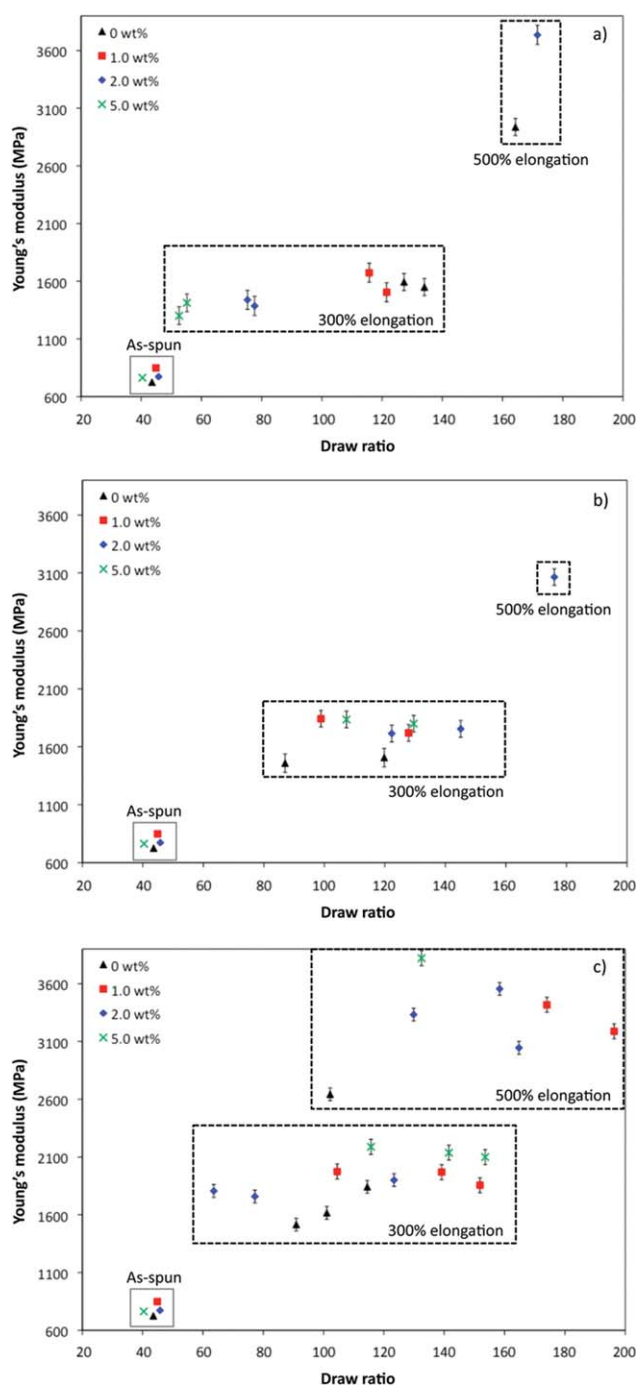


**Figure 8.** Average Young's modulus for MWNT/PA12 fibers postdrawn at (a) 100°C, (b) 120°C, and (c) 140°C. [Color figure can be viewed in the online issue, which is available at [wileyonlinelibrary.com](http://wileyonlinelibrary.com).]

GPa. Highest elastic moduli were obtained after 500% elongation for filaments containing 5.0 wt % (3.8 GPa), followed by 2.0 wt % (3.5 GPa) and 1.0 wt % (3.4 GPa).

Figure 8 demonstrated that the average Young's modulus generally increased when temperature and elongation increased as well. Parameters leading to the highest  $E$  values were 500% elongation and 140°C. Although several studies reported better

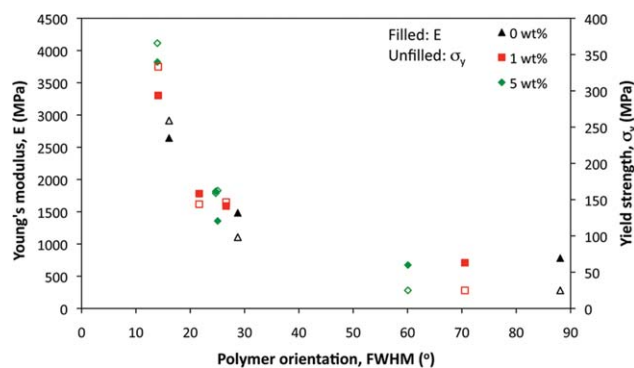


**Figure 9.** Effect of polymer chain orientation on average Young's modulus,  $E$ , and yield strength,  $\sigma_y$ , of postdrawn fibers containing 0, 1.0 and 5.0 wt % MWNT. The filled markers correspond to  $E$  and unfilled to  $\sigma_y$ . [Color figure can be viewed in the online issue, which is available at [wileyonlinelibrary.com](http://wileyonlinelibrary.com).]

mechanical properties with higher draw ratios, which compared well with the values presented in this article for the same matrix and type of nanofiller, postdrawing temperature was not identified as one of the key parameters.<sup>7-9,14-16</sup> During drawing, it was noticed that it was possible to stretch more filaments at higher speeds and elongation values at the highest temperature (140°C) and CNT weight fraction (5.0 wt %). This behavior was promoted by the softer nature of the matrix, allowing the polymer chains and nanotube network to move more easily. Lower crystallinity for fibers containing MWNT (Figure 6) might have also played an important role in their better drawability as the amorphous phase can dissipate more energy under tension.

It was previously presented in this article that postdrawing at 140°C led to the best polymer chains alignment (Figure 5). A comparison between elastic modulus, yield strength and the polymer chains orientation is shown on Figure 9 for fibers containing 0, 1.0, and 5.0 wt % MWNT. Both  $E$  and  $\sigma_y$  exhibit a similar trend and increase with polymer orientation. For FWHM above 20°, most of the properties improvements, if any, could be attributed to the chains orientation. However, the drastic increase below 20° shows that for this given level of alignment (attained after 500% elongation at 140°C), the addition of MWNTs played a noticeable part in achieving better mechanical properties, despite lower crystallinity. Similar findings were reported in the literature.<sup>10,28-30</sup> It was suggested that there must be some improvement in mechanical performance of the amorphous regions in the presence of CNT, notably that smaller crystals could connect those regions next to each other in a denser network.

## CONCLUSIONS

In this article, a postprocessing method to identify key parameters to improve mechanical properties of CNT/thermoplastic fibers was presented. A systematic investigation of the effects of drawing speed, temperature and elongation on the morphology and mechanical properties of the fibers was carried out. This work aimed to provide answers on the following points: (a) the effect of postdrawing parameters on the mechanical tensile

properties of MWNT/polyamide 12 fibers, and (b) the contribution of polymer chains alignment, crystallinity, and nanotubes alignment/dispersion on the improvement of these mechanical properties. It was observed that higher temperature (140°C) and elongation (500%) values had the greatest impact on Young's modulus and yield strength, but led to lower strain-to-failure values. These results were correlated to the alignment of the polymer chains. The drawing speed, within the values investigated, did not have a significant effect on the mechanical properties, but in an industrial framework, it would be preferable to use the highest speeds possible to increase productivity.

This postprocessing technique showed that the properties of CNT/thermoplastic fibers can be tailored according to specific parameters, depending on the requirements of the goal applications. It is expected that greater improvements could be obtained if this method were applied to other material systems and processing methods for the production of high performance fibers.

## ACKNOWLEDGMENTS

The authors like to acknowledge the Canada Research Chair (CRTI07-121RD project), McGill Engineering Doctoral Award and the National Research Council - Industrial Materials Institute (NRC-IMI, Boucherville, Canada) for their financial support and cooperation in this project. Arkema is also acknowledged for graciously providing materials, as well as Pierre Sammut, Nathalie Chapleau, Michel Carmel and Manon Plourde from NRC-IMI for their valuable input.

## REFERENCES

- Harris, P. J. F. *Carbon Nanotube Science: Synthesis, Properties And Applications*; Cambridge University Press: Cambridge, 2006.
- Nakajima, T. *Advanced Fiber Spinning Technology*; Woodhead Publishing Limited: Great Yarmouth, 1994.
- Salem, D. R. *Structure Formation in Polymeric Fibres*; Hanser: Munich, 2001.
- Dresselhaus, M. S. *Carbon Nanotubes: Advanced Topics in the Synthesis, Structure, Properties and Applications*; Springer: Berlin, 2008.
- Chawla, K. K. *Fibrous Materials*; Cambridge University Press: Cambridge, 1998.
- Chae, H. G.; Sreekumar, T. V.; Uchida, T.; Kumar, S. *Polymer* 2005, 46, 10925.
- Haggenmueller, R.; Du, F.; Fischer, J. E.; Winey, K. I. *Polymer* 2006, 47, 2381.
- Haggenmueller, R.; Gommans, H. H.; Rinzler, A. G.; Fischer, J. E.; Winey, K. I. *Chem. Phys. Lett.* 2000, 330, 219.
- Houphouet-Boigny, C. *Fiber reinforced polypropylene nanocomposites*. Ph.D. Thesis, Ecole Polytechnique Federale de Lausanne, Lausanne, Switzerland, 2007.
- Mazinani, S.; Aji, A.; Dubois, C. *Polym. Eng. Sci.* 2010, 50, 1956.

11. Sulong, A. B.; Park, J.; Azhari, C. H.; Jusoff, K. *Comp. Part B: Eng.* **2011**, *42*, 11.
12. Saeed, K.; Park, S.-Y. *J. Appl. Polym. Sci.* **2007**, *106*, 3729.
13. Saeed, K.; Park, S.-Y.; Haider, S.; Baek, J.-B. *Nanoscale Res. Lett.* **2009**, *4*, 39.
14. Perrot, C.; Piccione, P. M.; Zakri, C.; Gaillard, P.; Poulin, P. *J. Appl. Polym. Sci.* **2009**, *114*, 3515.
15. Anand, K. A.; Jose, T. S.; Agarwal, U. S.; Sreekumar, T. V.; Banwari, B.; Joseph, R. *Int. J. Polymer. Mater.* **2010**, *59*, 438.
16. Moore, E. M.; Ortiz, D. L.; Marla, V. T.; Shambaugh, R. L.; Grady, B. P. *J. Appl. Polym. Sci.* **2004**, *93*, 2926.
17. Dencheva, N.; Nunes, T. G.; Oliveira, M. J.; Denchev, Z. *J. Polym. Sci. Part B: Polym. Phys.* **2005**, *43*, 3720.
18. Fernandez, C. E.; Bermudez, M.; Alla, A.; Munoz-Guerra, S.; Tocha, E.; Vancso, G. *J. Polymer* **2011**, *52*, 1515.
19. Athreya, S. R.; Kalaitzidou, K.; Das, S. *Comp. Sci. Technol.* **2011**, *71*, 506.
20. Chatterjee, S.; Nuesch, F.A.; Chu, B.T.T. *Nanotechnology* **2011**, *22*, 275714.
21. Chatterjee, S.; Nuesch, F.A.; Chu, B.T.T. *Chem. Phys. Lett.* **2013**, *557*, 92.
22. Jose, M. V.; Steinert, B. W.; Thomas, V.; Dean, D. R.; Abdalla, M. A.; Price, G.; Janowski, G. M. *Polymer* **2007**, *48*, 1096.
23. Wang, W.; Murthy, N. S.; Chae, H. G.; Kumar, S. *Polymer* **2008**, *49*, 2133.
24. Minus, M.L.; Chae, H. G.; Kumar, S. *Polymer* **2006**, *47*, 3705.
25. Garcia-Gutierrez, M.C.; Nogales, A.; Rueda, D. R.; Domingo, C. *Polymer* **2006**, *47*, 341.
26. Sandler, J. K. W.; Pegel, S.; Cadek, M.; Gojny, F.; van Es, M.; Lohmar, J.; Blau, W. J.; Schulte, K.; Windle, A. H.; Shaffer, M. S. P. *Polymer* **2004**, *45*, 2001.
27. Zhou, C.; Wang, S.; Zhang, Y.; Zhuang, Q.; Han, Z. *Polymer* **2008**, *49*, 2520.
28. Mazinani, S.; Aji, A.; Dubois, C. *J. Polym. Sci. Part B: Polym. Phys.* **2010**, *48*, 2052.
29. Xie, L.M.; Aloys, K.; Zhou, X.P.; Zeng, F.D. *J. Therm. Anal. Calorim.* **2003**, *74*, 6.
30. Zhang, X.; Liu, T.; Sreekumar, T. V.; Kumar, S.; Hu, X.; Smith, K. *Polymer* **2004**, *45*, 8801.
31. Chávez-Medellin, R.; de Almeida Prado, L. A. S.; Schulte, K. *Macromol. Mater. Eng.* **2010**, *295*, 397.